ISOMERIC TRANSITIONS IN THE NEUTRON-RICH $N = 126$ REGION USING THE DESPEC SETUP AT GSI*

G. Bartram, Zs. Podolyák

on behalf of the S450 Collaboration

School of Maths and Physics, University of Surrey, Guildford, UK

Received 28 November 2024, accepted 7 February 2025, published online 10 April 2025

In May 2022 at the GSI Darmstadt, Germany, a ^{208}Pb beam at 1 GeV/u was used to populate neutron-rich fragmentation products at $N \approx 126$. Fragmentation products were separated and implanted in AIDA Si stoppers, surrounded by eight newly developed DEGAS and two EUROBALL high-purity Ge detectors. Delayed γ emissions revealed isomeric decays in ^{204}Pt, confirming previous findings. An isomeric half-life of 160 ± 30 ns was measured for the 10^+ state, and a combined half-life of 7.9 ± 1.3 μs for the 5^- and 7^- states. Additionally, approximately three times more ^{203}Ir events were detected than in 2006, suggesting new insights into the most neutron-rich $N = 126$ nucleus studied so far. Studying these nuclei enhances understanding of nuclear structure and nuclear shell models, and supports refining r-process path predictions for astrophysical isotopes.

DOI:10.5506/APhysPolBSupp.18.2-A24

1. Introduction

Approximately half of the observed heavy nuclei are connected to the astrophysical rapid neutron capture process (r-process). An elemental abundance peak at $A \sim 190$ is linked to neutron-rich $N = 126$ nuclei, where β^- decay begins to dominate over the capture of an additional neutron, forming waiting points on the r-process path [1]. It is not yet possible to perform direct measurements of these nuclei, therefore less neutron-rich $N = 126$ nuclei that are accessible through experimentation are observed instead. By performing γ-spectroscopy and measuring half-lives in the region shown by Fig. 1, further insight is given into current r-process predictions, as well as information on nuclear structure and potential shell evolution in exotic nuclei [2–4].

* Presented at the 57$^{\text{th}}$ Zakopane Conference on Nuclear Physics, *Extremes of the Nuclear Landscape*, Zakopane, Poland, 25 August–1 September, 2024.

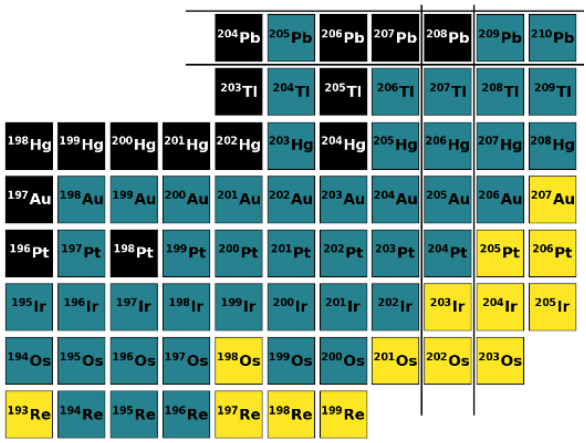

Fig. 1. (Colour on-line) A region of the chart of nuclides near neutron-rich $N = 126$ isotones. Black nuclei indicate stable nuclei. Blue/grey and yellow/light grey nuclei decay via β^- emission, with measured half-lives for those coloured blue/grey and unknown half-lives in yellow/light grey. Data from [5].

Most neutron-rich exotic nuclei in the $N = 126$ region can be produced by fragmenting ^{208}Pb. High-beam energy is essential to maximise electron stripping of the fragmentation products, enabling clear ion separation through a fragment separator. For this reason, the work was conducted at the GSI Helmholtzzentrum für Schwerionenforschung, where ^{208}Pb beams can be accelerated to 1 GeV/u [6]. The most sensitive method of studying exotic nuclei is by using isomeric (long-lived) states; if isomers survive the flight through the fragment separator ($\sim$ 300 ns), their decay can be detected.

The $N = 126$ nuclei, ^{204}Pt and ^{203}Ir, were studied via fragmentation at the GSI in 2006. In this experiment, the yrast structure of ^{204}Pt was determined up to $I = 10\hbar$ along with the half-life of 3 isomers [7]. In addition, 8,000 ^{203}Ir nuclei were recorded, allowing successful γ-spectroscopy and identification of one isomeric state [8]. The present work aims at improving the statistics for several $N \sim 126$ nuclei including ^{203}Ir in order to obtain new spectroscopic information. In these conference proceedings, the nuclear identification process will be described and the experimental method will be trialed by reproducing experimental results in ^{204}Pt.

2. Experimental setup

2.1. Beam production and fragment separator

The experiment took place at the GSI in May 2022 using a ^{208}Pb beam accelerated to 1 GeV/u by the UNILAC and SIS18 accelerator complex [9].

The beam was fragmented on a ^{9}Be target with a thickness of 2.512 g/cm^2. This was backed by an Nb foil to maximise the ionisation of the fragmentation products, which then entered GSI's fragment separator (FRS) (Fig. 2) consisting of several components used for ion separation and identification [10].

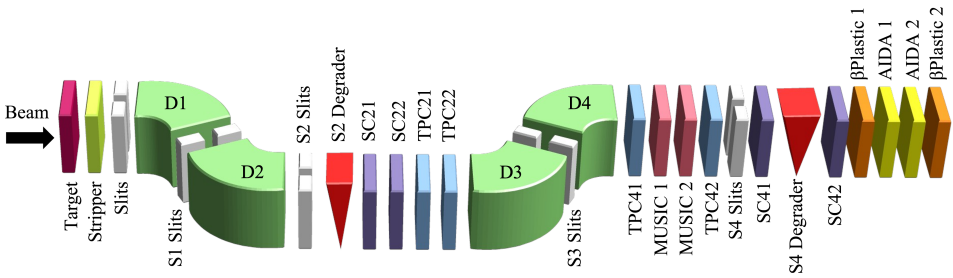

Fig. 2. (Colour on-line) A scheme of the fragment separator at GSI, highlighting the detectors used. The dipole magnets (D1–D4) are marked in green/grey.

In the mid-focal plane, an Al wedge degrader with a density of 4.5 g/cm^2 was operated in an achromatic mode to allow ion species to be separated by position along the final focal plane of the FRS. Four scintillation detectors and four time projection chambers (TPCs) were split between the S2 and S4 focal planes in order to perform time-of-flight (TOF) and position measurements, respectively. Two multi-sampling ionisation chamber (MUSIC) detectors were used to measure the energy loss of ions according to the Bethe–Bloch relationship ($\Delta E \propto Z^2$). A variable thickness Al degrader with an angle of 13 mrad was constructed for this experiment at S4 to ensure that ions were sufficiently slowed for implantation and to ensure optimal mean-range bunching. The dipole magnets were centered on ^{203}Ir and ^{202}Os for ~ 1 day and ~ 3 days, respectively.

2.2. Decay spectroscopy

After passing through the FRS, the fragmentation products entered the decay spectroscopy (DESPEC [11]) setup where they were implanted in the advanced implantation detector array (AIDA) consisting of two layers of double-sided Si strip detectors (DSSDs). AIDA was used in the 24×8 cm^2 wide configuration comprising of 384×128 pixels for precise implant and β-decay tagging. Two β-plastic detectors with the same dimensions were placed either side of the AIDA stack, allowing for correlation between detected β-particle emission and time of ion implantation in AIDA. The β-plastic detectors and AIDA DSSDs were contained within the AIDA Snout (Fig. 3 (left)), which was surrounded by an HPGe array, consisting

of 38 crystals for γ-spectroscopy (Fig. 3 (right)). The array was made of 2 well-established EUROBALL clusters with 7 crystals each, and the 8 newly developed DEGAS detectors with 3 crystals each. A unique feature of the DEGAS detectors is their narrow cryogenic cooling cylinders which allow them to be tightly packed for optimal solid angle coverage. This was the first use of the DEGAS array, in preparation for use at future FAIR experiments [12].

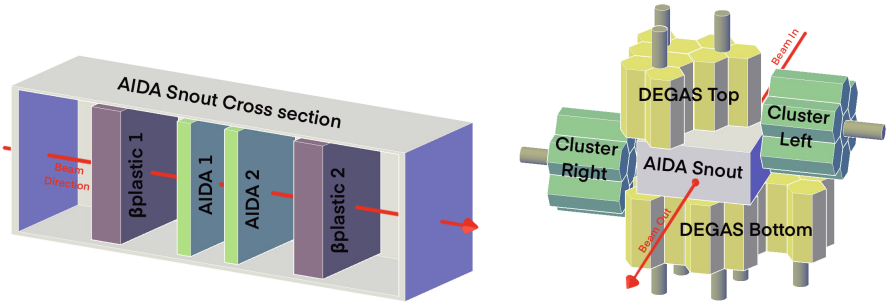

Fig. 3. Left: A schematic showing the cross section of the AIDA Snout, containing two AIDA DSSDs and two β-plastic detectors. Right: A scheme of the HPGe setup, featuring 8 DEGAS and 2 EUROBALL cluster detectors.

3. Identification

Several techniques were utilised to identify the fragmentation products. Corrections were made for the drift in energy loss measurements from the MUSIC detectors over time. Furthermore, corrections for angular dispersion in the mass–charge ratios (A/Q) were applied for each ion species in both settings. This increased the precision of the Z and A/Q separation for individual ions. Due to the nature of high-mass nuclei, nuclei in different charge states were present in the identification plots. By plotting the change in energy in the S2 degrader against the proton number (Z) value of the fragmentation products, the charge states were separated, as shown in Fig. 4.

Since the S2 degrader was operated in the achromatic setting, the fragmentation products were separated by position in the S4 focal plane ($X4$). The subsequent $X4$ *versus* A/Q plots yield more distinct isotope separation than Z *versus* A/Q for the same data; therefore, the $X4$ data was used for identification. Figure 5 shows that by gating on only the $\Delta Q = 0$ nuclei, the number of overlapping kinematic loci was reduced, resulting in a clean identification plot which was used to assign nuclei. To ensure each ions' accurate assignment, the $X4$ and A/Q values for each isotope cluster were cross-checked with LISE++ simulations. In addition, γ-spectroscopy of nuclei with strong previously identified isomeric transitions (such as ^{204}Pt) were used to confirm the identification.

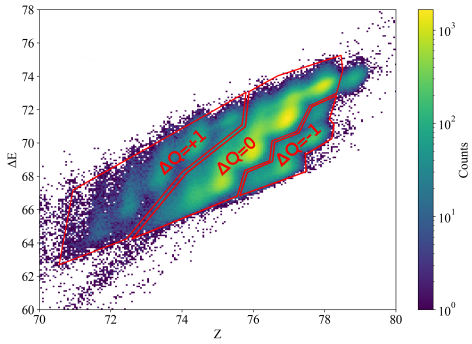

Fig. 4. Energy loss in the S2 degrader against Z value for charge state separation. $\Delta Q = 0$ refers to ions that maintain the same number of electrons throughout the separator, $\Delta Q = -1$ referring to nuclei that have picked up an electron, and $\Delta Q = +1$ to those that have lost one electron at S2.

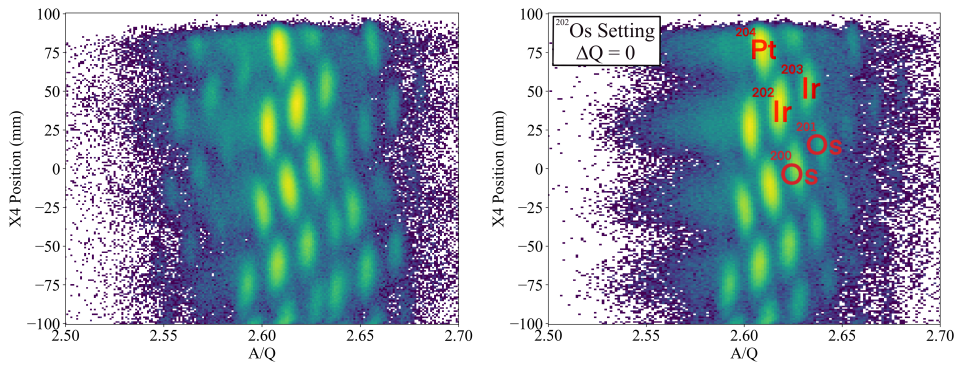

Fig. 5. Plots that highlight the effect of charge state separation on S4 focal plane position *versus* A/Q identification. Left: All data in the ^{202}Os setting with no charge state selection. Right: The same data gated only on $\Delta Q = 0$ nuclei.

4. Results and discussion

After charge state selection and nuclear assignment was undertaken for both the ^{202}Os and ^{203}Ir settings, the number of each isotope produced was totaled across all charge states. Table 1 shows the number of events identified for some of the key nuclei. Notably, 23,000 ^{203}Ir nuclei were produced compared to 8,000 ions in the 2006 experiment [8].

An example spectrum was produced using data from the HPGe detectors for ^{204}Pt nuclei across both settings and multiple charge states (Fig. 6). The spectrum shows that the 872 and 1123 keV appear with greater statistics when a long timing condition is applied, whereas the 1061 and 1156 keV

appear with approximately the same number of counts in both the long and short timing conditions. This indicates the presence of both a long-lived and short-lived isomer which were previously reported by Steer [7].

Table 1. A table detailing the number of events identified for some of the key nuclei produced.

Isotope	Number identified
^{204}Pt	135,000
^{203}Ir	23,000
^{202}Ir	84,000
^{202}Os	hundreds
^{201}Os	5,000
^{200}Os	26,000

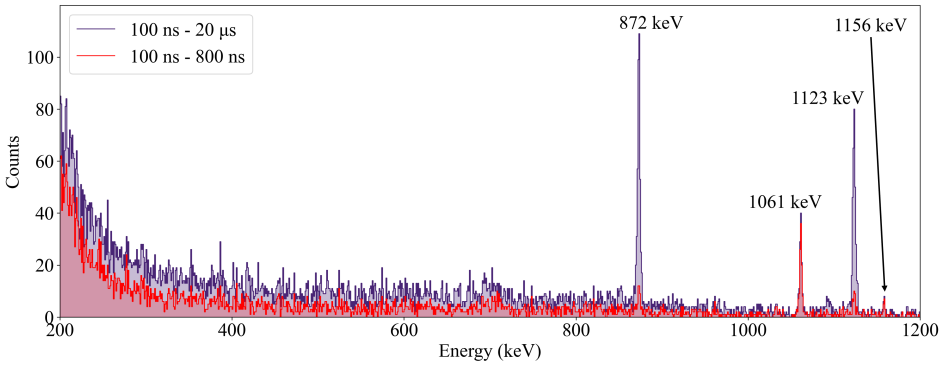

Fig. 6. (Colour on-line) A spectrum of ^{204}Pt showing previously established γ rays, with two different timing parameters to distinguish between long-lived purple/(black) and short-lived (red/grey) isomers.

For the long timing condition (100 ns–20 μs after implantation), the 872 and 1123 keV peaks were used to calculate the half-life of the reported 5^- isomer, as shown in Fig. 7 (left). The same was done for 10^+ isomer using the 1061 and 1156 keV peaks with the short timing condition (100–800 ns) producing Fig. 7 (right).

Notably, a low-energy γ transition with a half-life of 55 ± 3 μs is also reported to occur from the 7^- to the 5^- state. However, the hardware for this experiment limited the timing correlation to 20 μs, meaning that the longer-lived decay component could not be fitted. Therefore, only one isomeric half-life including both 5.5 and 55 μs elements was determined, giving a disparity between this experiment's value and the literature. The

isomeric half-life was calculated to be 7.9 ± 1.3 μs for the 5^- state, compared with 5.5 ± 0.7 μs in the literature; the 10^+ state was calculated to have a 160 ± 30 ns half-life, which is in excellent agreement with the previously reported value of 146 ± 14 ns [7].

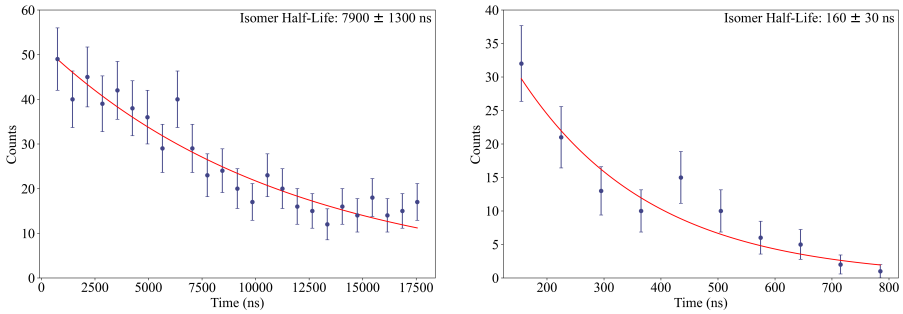

Fig. 7. Left: The decay of the 5^- state. Right: The decay of the 10^+ state.

5. Conclusions

The output of this experiment shows the successful production and identification of several nuclei in the $N = 126$ region, where the example of ^{204}Pt has been presented to show how γ-spectroscopy can be used to study the structure of nuclei. Approximately three times the number of ^{203}Ir events have been recorded compared to in 2006, suggesting that new information can be obtained on the most neutron-rich $N = 126$ nucleus studied to date.

REFERENCES

[1] E.M. Burbidge *et al.*, *Rev. Mod. Phys.* **29**, 547 (1957).
[2] J.J. Cowan *et al.*, *Rev. Mod. Phys.* **93**, 015002 (2021).
[3] K.-L. Kratz *et al.*, *Astrophys. J.* **403**, 216 (1993).
[4] Q. Zhi *et al.*, *Phys. Rev. C* **87**, 025803 (2013).
[5] B. Pritychenko *et al.*, *Nucl. Instrum. Methods Phys. Res. A* **640**, 213 (2011).
[6] M. de Jong *et al.*, *Nucl. Phys. A* **628**, 479 (1998).
[7] S.J. Steer *et al.*, *Phys. Rev. C* **78**, 061302 (2008).
[8] S.J. Steer *et al.*, *Phys. Rev. C* **84**, 044313 (2011).
[9] K. Blasche *et al.*, *IEEE Trans. Nucl. Sci.* **32**, 2657 (1985).
[10] H. Geissel *et al.*, *Nucl. Instrum. Methods Phys. Res. B* **70**, 286 (1992).
[11] A.K. Mistry *et al.*, *Nucl. Instrum. Methods Phys. Res. A* **1033**, 166662 (2022).
[12] G.S. Li *et al.*, *Nucl. Instrum. Methods Phys. Res. A* **890**, 148 (2018).